# Climate sensitivity to changes in ocean heat transport

Marcelo Barreiro

*Unidad de Ciencias de la Atmosfera, Facultad de Ciencias, Universidad de la Republica, Uruguay*

Annalisa Cherchi and Simona Masina

*Centro Euro-Mediterraneo per i Cambiamenti Climatici, and Istituto Nazionale di Geofisica e Vulcanologia, Bologna, Italy*

Revised for J. Climate on April 19th, 2011

*Author address:* Marcelo Barreiro, Unidad de Ciencias de la Atmósfera, Instituto de Física, Facultad de Ciencias, Universidad de la República, Igua 4225, Montevideo 11100, Uruguay. *Tel: +5982 5258624, Fax: +5982 5250580, Email:* barreiro@fisica.edu.uy

## Abstract

Using an atmospheric general circulation model coupled to a slab ocean we study the effect of ocean heat transport (OHT) on climate prescribing OHT from zero to two times the present-day values. In agreement with previous studies an increase in OHT from zero to present-day conditions warms the climate by decreasing the albedo due to reduced sea-ice extent and marine stratus cloud cover and by increasing the greenhouse effect through a moistening of the atmosphere. However, when the OHT is further increased the solution becomes highly dependent on a positive radiative feedback between tropical low clouds and sea surface temperature. We found that the strength of the low clouds-SST feedback combined with the model design may produce solutions that are globally colder than Control mainly due to an unrealistically strong equatorial cooling. Excluding those cases, results indicate that the climate warms only if the OHT increase does not exceed more than 10% of the present-day value in the case of a strong cloud-SST feedback and more than 25% when this feedback is weak. Larger OHT increases lead to a cold state where low clouds cover most of the deep tropics increasing the tropical albedo and drying the atmosphere. This suggests that the present-day climate is close to a state where the OHT maximizes its warming effect on climate and pose doubts about the possibility that greater OHT in the past may have induced significantly warmer climates than that of today.

## 1. Introduction

The oceans absorb heat mainly in the tropical regions where cold water upwells to the surface and lose it in high latitudes where cold and dry winds blow over warm currents during winter time. This implies a net heat transport by the oceanic circulation from the equator to the polar regions that contributes to remove the surplus of heat received in the tropics. Averaged over long times the ocean must gain and lose equal amounts of heat in order to maintain a steady state. The oceanic heat transport is largest in the tropical region and becomes very small poleward of 45° (Trenberth and Caron 2001). At higher latitudes the heat transported by the atmosphere, due mainly to the presence of energetic eddies, is the main contributor to total poleward heat transport.

The circulation of the oceans likely changed over the course of Earth's history, due to changes in external forcings, e.g, insolation and greenhouse gases, and changes in continental configuration. Thus, a change in ocean heat transport is a common explanation in studies of past climates. For example, Rind and Chandler (1991) propose that 46% greater ocean heat transport during the Jurassic period (200-144 million years ago, Ma) would have warmed the climate by 6 K. They also suggest that 68% greater ocean heat transport during the Cretaceous (144-65 Ma) would have warmed the climate by 6.5 K. Barron et al. (1993) studied the impact of oceanic heat transport in the Cretaceous using an atmospheric model coupled to a slab ocean. Imposing present-day zonally averaged heat transport but distributed differently among oceans due to a different continental configuration they found that increased ocean heat transport warms the climate. Moreover, they found that the warming is not linearly related to the value of oceanic heat transport: increasing from 0 to present day heat transport increases the surface temperature by 2.6 K, but only 0.6 K from present day to two times present day values. Closer to the present and already with the same continental configuration, Dowsett et al. (1996, 2009) argue that the warmer high latitude ocean temperatures during the mid-Pliocene (~3 Ma) can be explained by a more vigorous North Atlantic Deep Water formation and thermohaline circulation. Finally, Romanova et al. (2006) found using an atmospheric general circulation model that reduced ocean heat transport contributed to global cooling during the Last Glacial Maximum. In general, patterns of decreased equator-to-pole temperature gradients due to a large extratropical warming, as in the case of the Eocene, are explained as due to enhanced ocean heat transport (Barron 1987, Zachos et al 1994, Emanuel 2002): larger ocean heat transport decreases sea ice in high latitudes leading to an ice-albedo feedback that warms these regions. The tropics may cool or stay close to present values, so that there is overall global warming. In recent years, other studies have suggested that increased ocean heat transport cannot fully explain the decrease in the meridional temperature gradient during the Eocene (Huber and Sloan 2001). Alternative explanations involving high latitude convection feedbacks have been proposed to explain the high latitude warming of past climates (Abbot and Tziperman 2008).

The undergoing changes in climate caused by human activities will probably affect the oceanic circulation and its heat transport, which then may feed back onto the atmosphere and climate. Nevertheless, the connection between atmospheric and oceanic heat transports is not yet well understood. For example, is it possible to change one component without changing the other one? Everything else being equal (e.g. constant greenhouse concentration), this would result in changes in the albedo of the planet because the total heat transport by the ocean-atmosphere system will be different, and thus the system has to gain heat differently at each latitude.

The work of Stone (1978) argues that the characteristics of internal ocean-atmosphere dynamics have little effect on the total (ocean+atmosphere) poleward heat transport. He argues that the total heat transport depends only on the solar constant, the axial tilt of the planet, the radius, and the albedo, and thus the total heat transport depends only on external factors. The reasoning behind is that as the temperature of the planet increases the albedo declines and the outgoing longwave radiation increases, thus avoiding large changes in radiative fluxes. Therefore, no large changes in energy fluxes across latitudes are necessary to balance this heating (see also Barron 1987),implying a large compensation between the heat transported by the oceans and the atmosphere. This argument has lead people to believe that it is easier to change one component of the heat transport rather than the total. Changes in continental distribution makes changes in ocean heat transport an easy target to explain past climate changes.

A recent study by Enderton and Marshall (2009) explores the Stone (1978) argument using a coupled ocean-atmosphere model and imposing different simplified “continental” configurations. Their results largely agree with that of Stone (1978), but they also suggest that the total heat transport will depend on the meridional gradient of the albedo. In this study changes in the tropical band are very small, probably due to the use of very simple cloud dynamics of the model. Particularly, the atmospheric model they used does not have a parameterization for stratus clouds and the albedo is directly proportional to the total cloud cover. Barreiro et al. (2006) showed that this simple cloud parameterization gives opposite results to those of state-of-the-art atmospheric models when forced with prescribed tropical sea surface temperature patterns that are different from those of the present-day.

The representation of clouds is one of the main weaknesses of current climate models (Bony et al. 2006). In particular, the parameterization of boundary layer stratus clouds has proved to be very difficult and has been a major area of research in the last decade. These clouds have a very weak greenhouse effect, but strongly reflect incoming shortwave radiation, thus modulating the albedo of the Earth. Bony and Dufresne (2005) have shown that the simulation of marine low level clouds is a large source of uncertainty in tropical cloud feedbacks and of climate sensitivity, suggesting that the simulation of tropical responses to different forcings will strongly depend on the parameterization of these clouds, and that results need to be tested using different cloud schemes.

The papers by Winton (2003, hereafter W03) and Herweijer et al. (2005, hereafter H05) explore the mechanisms through which ocean heat transport warms the climate using atmospheric general circulation models coupled to fixed oceans where the heat transport can be imposed. H05 studied the difference between experiments with zero ocean heat transport versus that of present day heat transport. W03 used coupled models with fixed currents and studied the difference between runs with ocean currents changed to 50% and 150% from present day conditions. Overall, these studies found that the ocean heat transport warms the climate by 1-3.5 K depending on the model and the configuration. W03 found that increased ocean heat transport reduces sea-ice extent and the low oceanic cloud cover in tropics and midlatitudes, thus reducing the albedo of the planet. H05 further showed that ocean heat transport increases the clear-sky greenhouse trapping due to moistened subtropics. This positive “dynamical-feedback” results from a change in the atmospheric circulation that both redistributes the water vapor and allows for a global atmospheric moistening. H05 also found that the atmosphere tends to compensate for changes in oceanic heat transport, as Stone (1978) suggested. In the deep tropics, where the ocean heat transport is largest, the compensation is almost complete, while elsewhere the total heat transport is slightly larger when the ocean transports heat.

The studies by W03 and H05 suggest that further increasing the OHT from today's conditions will further warm the climate. This is supported by the work of Barron et al. (1993) mentioned above. In this study we revisit the results of W03 and H05 and, having in mind paleo-climates, we extend the study by increasing values of ocean heat transport beyond present day conditions. In this way we intend to address more completely the question of the role of ocean heat transport in climate. Consistent with the above discussion we test the sensitivity of the results to two different cloud schemes. In agreement with previous studies we found that an increase in OHT from zero to present-day conditions warms the climate. However, when the OHT is further increased the solution becomes highly dependent on a positive radiative feedback between tropical low clouds and sea surface temperature.

The study is organized as follows: section 2 is a description of the model and of the experimental setup. Section 3 shows the main results of the study, and section 4 discusses their plausibility, because the strength of the low clouds-SST feedback combined with the model design may produce solutions with unrealistically strong equatorial cooling. Section 5 presents a diagnosis of the behavior of the tropical response and its adjustment. Finally, section 6 concludes the study summarizing the results, and discussing their implications and shortcomings.

## 2. Model and experiments

As in the study of H05 we use an atmospheric model coupled to a slab ocean. This configuration has the advantage of allowing the prescription of ocean heat transport, thus facilitating the study of its role in climate. The slab ocean allows air-sea thermodynamic interactions, but does not allow the ocean to adjust dynamically to changes in the wind stress. Since changes in the surface stress may provide a (positive/negative) feedback that is not realized in the model, the solutions presented in this study have to be further tested in a coupled model configuration. In spite of this caveat, we still believe the results presented here are very relevant to understand the climatic response to a change in the ocean heat transport. This should be particularly true for small perturbations from present day conditions.

The atmospheric general circulation model used in the present study is the fifth generation of the ECHAM model. We used ECHAM5 in its standard resolution with an horizontal grid of 2.8125°x2.8125° (T42) and 19 vertical levels and standard physics (Roeckner et al. 2003).

ECHAM5 is coupled to a motionless slab ocean 50 meters deep, whose equation is

$$C_O \frac{\partial SST}{\partial t} = Q_A + Q_{Oc}$$

where *SST* is the sea surface temperature, $C_O$ is the heat capacity of the ocean, $Q_A$ is the net atmospheric heat flux (turbulent plus radiative fluxes), and $Q_{Oc}$ is a fixed (heat flux divergence) term that represents the climatological ocean heat transport that is included in order to simulate correctly the present seasonal cycle of sea surface temperature. The $Q_{Oc}$ is calculated from the surface heat fluxes of a run in which the atmospheric model is forced with prescribed climatological sea surface temperature, resolving the seasonal cycle, and sea-ice. To assure a balanced oceanic heat budget the global average of $Q_{Oc}$ is set to zero. Prescription of the $Q_{Oc}$ allows imposing different ocean heat transports to the atmosphere. In this study we imposed to the atmospheric model the following heat transports:

$$OHT = cQ_{Oc}, \quad c = (0, 0.5, 0.75, 1, 1.25, 1.5, 2)$$

Thus, we maintain the present-day spatial structure of the regions where the oceans gain and lose heat, but multiply it by a factor c at each grid point in order to simulate a decreased/increased oceanic heat transport. For example, c=1 is the Control case with present-day ocean heat transport; c=1.5 represents a case where the ocean heat transport is 50% larger than today's conditions (see Fig. 1). The results of the experiments when c < 1 (ocean heat transport is reduced) are directly comparable to those of W03 and H05. Each experiment is run for 40 years. The model typically adjusts in less than 20 years, and we use the average of the last 10 years to compare the climates of the different experiments.

Alternatively, we could have changed the regions where the oceans gain and lose heat, which would represent a drastic change in the circulation. Since we do not have much guidance about the patterns of surface heat fluxes for different configurations of the ocean circulation we decided against this alternative. Moreover, since the ocean heat budget needs to be balanced, decreasing the uptake of heat in one region would imply the decrease in the heat loss in a different region, with a possible dependence of the solution on the chosen region.

By experimental design, in climatological sea-ice areas the ocean heat flux is set to zero. But, if new sea-ice is forming (e.g. in areas free from it in the Control experiment), the ocean heat flux is taken into account in the calculation of the sea-ice thickness. In the model, when new sea-ice forms or melts the changes in the surface heat fluxes are taken into account and the OHT changes accordingly. Nevertheless, a full coupling is missing and changes in the OHT do not fully realize its impact on the sea-ice weakening the ice-albedo feedback and thus the extratropical warming. Moreover, the absence of a land-ice model does not allow the continental glaciers to change in extent thus providing another limiting effect to the extratropical cooling.

In order to test the sensitivity of the results to cloud parameterization we perform the experiments described above using two different schemes. The default cloud cover scheme in ECHAM5 is that of Tompkins (2002). This is a statistical scheme based on prognostic equations for the moments (skewness and width) of the probability distribution function for the total mixing ratio $r$, $G(r)$. Given $G(r)$ the fractional cloud cover $C$ is calculated as $C=\int_{r_s}^{\infty} G(r)\,dr$, where $r_S$ is the saturation mixing ratio. The equations for the moments of the distribution take into account the effect of unresolved turbulent fluctuations, convection and microphysical processes (Roeckner et al. 2003).

ECHAM5 has an alternate diagnostic scheme for cloud cover based on Sundqvist et al. (1989). If $RH$ is the grid mean relative humidity, the fractional cloud cover $C$ in this scheme is calculated as

$$C=1-\sqrt{1-b_0}, \quad b_0=\frac{RH-RH_0}{1-RH_0},$$

where $RH_0$ is a condensation threshold that depends on height (see also Lohmann and Roeckner 1996). The microphysics parameterizations are the same for both of the schemes considered.

In the following we consider the tropical region as that defined loosely between 30°S and 30°N, the equatorial region as that bounded by 10°S-10°N, and the subtropics as the regions between 10°-30°.

## 3. Results

Figure 2a (black line) shows the global mean surface temperature for the experiments with changed oceanic heat transport using the default prognostic cloud scheme. For decreased OHT, as the model moves from zero to present-day values, the mean effect of the ocean circulation is to warm the climate. W03 and H05 obtained similar results, albeit with smaller sensitivity. However, according to our model, if the OHT increases further from present-day values it would cool the global climate. Moreover, it shows large sensitivity to relatively small changes: a 25% increase in OHT cools the climate by more than 4 K (Fig 2a). Further increases (beyond 25%) would also cool the climate but more gradually. The transition from a warming to a cooling effect of increased OHT is not gradual but abrupt. In order to better resolve this transition we run additional experiments for c=1.05, 1.1, 1.15, and 1.20. Results show that the occurrence of a warmer climate with increased OHT is valid for c<1.15, that is for less than a 15% increase in the present-day values. Thus, in this model, the current climate is such that the ocean heat transport is close to its maximum positive influence.

Top of the atmosphere radiation fluxes show that after 40 years the model has reached equilibrium for all experiments except for the case of zero oceanic heat transport where there is excess outgoing longwave radiation compared to incoming shortwave meaning that the climate will cool further (Fig. 2b). According to the incoming shortwave radiation, changes in the ocean heat transport can significantly alter the albedo of the planet, that has a minimum for c=1.10. Total cloud cover accompanies these changes in albedo (Fig. 2c). The mean surface temperature as well as the changes with respect to Control for a 50% change in oceanic heat transport are shown in Figure 3. Clearly, the areas of large temperature changes are different according to the sign of the heat transport changes: for decreased ocean heat transport the largest changes (cooling) are in the high latitudes (Fig. 3c), in agreement with previous studies (W03). For increased ocean heat transport the largest changes are over the tropical oceans where surface cooling reaches over 25 K (Fig. 3d). In this latter case the high latitudes also cool, except for small areas next to the Kuroshio Current and in the North Atlantic.

The large cooling in the eastern Pacific for a 50% increase in OHT is such that the surface temperature becomes less than 0 °C. A heat budget analysis of the cold tongue region reveals large changes in the surface fluxes except for the sensible heat (Fig. 4, red line). The main contributor to the cooling is a large reduction of the incoming shortwave radiation at the surface (Fig. 4c), which is accompanied by a decrease in the upward release of latent heat (Fig. 4a) and of long wave radiation (Fig. 4d). These changes occur on a time scale of 10 years and, as we will see below, it is a consequence of a large increase in the amount of highly reflective low clouds in the equatorial region. On the contrary, for a reduction in the OHT (c=0.5) the net surface short wave radiation does not change (Fig. 4c, blue line), but there is an increase in the turbulent fluxes (Fig. 4a,b blue line) and in the long wave radiation (Fig. 4d, blue line) concordant with a warming of the cold tongue region (Fig. 3c).

In agreement with previous studies we found that the high latitudes cooling for decreased OHT is accompanied by increased low level clouds (defined as those within 1000-700 mb) with a maximum at about 40°N (Fig. 5c). Moreover, the smaller the ocean heat transport, the more low clouds are created in the northern extratropics. As the low clouds are highly reflective, the experiments with reduced OHT have a higher albedo in high latitudes that results in less incoming shortwave radiation (Fig. 5a). In low latitudes cloud changes are small, and so are shortwave radiation changes. Also, in these experiments the high latitude cooling moves the -1.8°C isotherm equatorward in both hemispheres allowing for large increases in sea-ice that result in an increase of reflected shortwave at the surface (Figs. 5b,d). All these processes tend to increase albedo and have a cooling influence on climate.

The climatic changes for increased OHT are very different. In this case, the extratropical low clouds show a slight decrease (Fig. 5c) that, by allowing more incoming shortwave radiation (Fig. 5a), would warm the climate. However, there are large changes in the tropical low clouds (Fig. 5c) that overwhelm those changes. As the oceanic heat transport increases the amount of low clouds in deep tropical regions increases enormously, which is also seen as a large increase in the amount of reflected shortwave radiation at the top of the atmosphere (Figs. 5a,c). A 50% increase in OHT results in a 40 W/m$^2$ increase in reflected shortwave radiation at the top of the atmosphere. This has a large cooling influence evidenced particularly by the large oceanic cooling in the equatorial Pacific (Fig.

3b,d). Clearly, these changes result from a positive feedback between SST and low level clouds: an increase in oceanic heat transport induces a tropical cooling which creates more stratus, which then cool the SST further, and so on. In this model the SST-stratus feedback seems to be quite strong. The northern hemisphere cooling is further evidenced by small changes in sea ice, with weak increases in the experiments with c=1.25 and c=1.5, and a weak decrease in the experiment with c=2 (Fig. 5d).

We next look at changes in the greenhouse trapping, defined as the difference between the upward longwave radiation at the surface and that at the top of the atmosphere. The more optically thick is the atmosphere, the larger the greenhouse trapping and the greenhouse effect. Changes in the greenhouse effect can be either due to clouds or to water vapor content in the atmosphere. To separate between cloud and clear-sky effect we plot total greenhouse trapping as well as clear-sky greenhouse trapping, and their difference (fig. 6a,c,d). We also plot total column water vapor (Fig. 6b).

For both increased (actually, $c>1.10$) and decreased OHT the atmosphere tends to become drier than the Control case, and it is mainly a clear-sky effect (compare Figs. 6a,c). However, the changes occur in different regions. As in the case of shortwave radiation, the changes in greenhouse trapping occur mainly in the northern high latitudes for decreased OHT, and in the tropics for increased OHT. For increased OHT the tropics become very dry as evidenced by huge changes in the total integrated water vapor (Fig. 6b). Changes in the cloud cover play a secondary role, but it is possible to distinguish two regions at 20°N, S where there is increased greenhouse trapping and a decrease in the equator (Fig. 6d), signaling the creation of two Intertropical Convergence Zones at 20°N,S. For decreased OHT the cloud effect also marks a shift of the ITCZ to south of the equator (Fig. 6d).

The changes described above are integrated in the heat transported by the ocean+atmosphere system (Fig. 7). We found that for values of the OHT smaller than present-day, the atmosphere tends to almost perfectly compensate in the deep tropics, but does not compensate completely in the extratropics so that the total heat transported at about 35°N is ~ 0.5PW (depending on c) smaller than in the Control case (Fig. 7a). For values of OHT larger than a 10% increase the total heat transported by the ocean+atmosphere system decreases at all latitudes (Fig. 7a), and particularly in the tropics because the atmosphere transports heat equatorward in both hemispheres (Fig. 7c).

Overall, our results confirm the study of H05 for OHT smaller than present day. Moreover, we have found that increases in the OHT larger than 10% of present-day values lead to a cooling mainly due to a) an increase in the low level tropical clouds that increases the albedo and reflect more incoming shortwave radiation, and b) a large drying of the tropical region that reduces the greenhouse trapping. Different than for the case of smaller OHT, the cases for larger OHT involve significant changes in the tropical clouds, particularly in the low level marine stratus clouds, and their interaction with the sea surface temperature. Since the parameterization of stratus clouds is one of the main weaknesses of current atmospheric models we tested the sensitivity of the results using the alternate diagnostic parameterization for cloud cover (see Section 2) with a similar set of runs. The new results are shown as red curves in Fig. 2. Overall the results are qualitatively similar as for the prognostic scheme, that is, the climate cools for decreasing or increasing the ocean heat transport. Moreover, the behavior of the total cloud response and top of the atmosphere fluxes is similar for both schemes. However, it can be seen that the climate sensitivity to changes in OHT is lower using the diagnostic scheme and the warmest climate occurs for a 25% increase when climate becomes 0.6 K warmer (Fig. 2a, red line). Moreover, differences between schemes are relatively small for c<1.15, but significant for larger values of c. This is further illustrated in the spatial amplitudes of the surface temperature changes (Fig. 8). While the amplitudes of the changes in surface temperature for a 50% decrease in OHT are comparable (Fig. 3c vs Fig. 8a), that is not the case for a 50% increase (Fig. 3d vs Fig. 8b). The large tropical cooling seen in Fig. 3d has been largely reduced in Fig. 8b and that has global implications: while using prognostic clouds the extratropics cool almost everywhere, using diagnostic clouds the high latitudes become warmer for a 50% increase. This surface temperature pattern is closer to what previous studies (e.g. Dowsett et al 2009) have assumed about the effect of an increase in OHT. However, even in this case (50% increase in OHT), the global climate cools by 1 K with respect to present-day conditions.

**4. Physical plausibility of the results**

The results presented in the previous section are a priori very surprising because the current understanding is that an increase in ocean heat transport tends to warm the climate, which also agrees with other studies using previous atmospheric models, like those of Rind and Chandler (1991), or Barron et al. (1993). This last study, in particular, finds that using an atmospheric model with physical parameterizations simpler than those used in this study a doubling of the ocean heat transport still warms the climate. However, the authors noticed that the relationship between climate and the heat transport is nonlinear: climate warms by 2.6 K from 0 to present-day heat transport, but only 0.6 K from present-day to two times present-day heat transport.

Some of the experiments presented in this study are not very realistic and pose doubts not only about their implications  but also in general about the use of mixed-layer models to study climate sensitivity under different conditions. In particular, in the experiment with prognostic clouds and a 50% increase in OHT the temperature of the Pacific cold tongue is close to the freezing point and is colder than that of the subtropics, something that is not likely to happen in the real world. As mentioned before, the experimental setup used in this study does not allow the ocean to adjust dynamically to the changes in the winds and thus can not act as a negative feedback opposing the positive SST-clouds radiative feedback. This is likely the reason why the cold tongue cools enormously to the point of having near-freezing temperatures. In a steady state the temperature of the cold tongue region is controlled by the temperature of the subducting waters in the subtropics. Moreover, it would not be possible to transport heat polewards if the equatorial waters are colder than the subtropics. Thus, the results are physically plausible up to the limit when the tropical meridional temperature gradient becomes zero, that is, when the tropics are widest.

Therefore, in order to check the plausibility of the solutions we computed the meridional SST difference in the tropical Pacific, defined as the SST average over [120°E-100°W, 10°S-10°N] minus that over [120°E-100°W, 10°N-30°N], as a function of the strength of the OHT (in terms of parameter c). We also calculated the zonal equatorial SST difference, defined as the SST average  in the region [150°E-165°E, 5°S-5°N] minus that over [100°W-85°W, 5°S-5°N].

We found that for prognostic clouds the meridional SST difference is positive for $c<1.15$, while for diagnostic clouds this is true for $c<=1.25$ (Fig. 9). Thus, the physically plausible solutions are those for a relatively small increase in OHT and depend on the cloud scheme used. These solutions are such that an increase in OHT has a warming effect on climate, independently of the cloud scheme. Moreover, for $c<1.15$ the dependence of the meridional difference on c is very similar in both cloud schemes, showing a decrease with increasing OHT. Coincident with the global effect on climate, for c between 1.1 and 1.15 the prognostic scheme shows an abrupt transition in the behavior of the meridional difference changing from +1.5 K to more than -2.0 K. After the transition the meridional difference keeps decreasing with increased c with a more gradual slope, similarly to the diagnostic case.

The zonal SST difference increases with increasing OHT (Fig. 9a). The behavior is similar using prognostic or diagnostic schemes until $c=1.1$; after that value there is an abrupt increase in the difference for the prognostic cases concomitant with the change in sign of the meridional difference. On the other hand, for the diagnostic scheme there is an approximately linear increase in the zonal SST difference for all values of c. The prognostic scheme is so sensitive to change in OHT that for c=2 all the tropics are covered by stratus and the equatorial region cools uniformly. According to these results it is not possible for the tropical region to be broad and have a decreased equatorial east-west SST gradient at the same time, a situation that apparently occurred during the mid-Pliocene (Fedorov et al 2006, Brierley et al 2009). It is worth pointing out, however, that the present work is limited by its assumption that the OHT has a pattern like that of today with varying amplitude, and thus ignores possible changes in the spatial pattern of OHT that may have occurred in the past.

We have found that the maximum warming effect of the OHT on climate corresponds to the situation when the tropical region is widest, and it coincides with the limit of physically plausible solutions. Moreover, this limit is highly dependent on the cloud scheme, which sets the strength of the SST-clouds radiative feedback within the tropics. In the next section we analize more closely the behavior of the tropical clouds to changes in OHT in order to understand the processes involved.

**5. Diagnosing the tropical response**

We base our discussion on the ideas proposed by Klein and Hartmann (1993), Miller (1997), and Clement and Seager (1999), among others, relating atmospheric low-level stability and clouds to sea surface temperature. The basic assumption is that an ocean region can be divided into a cold pool and a warm pool. In our case, the warm pool refers to the equatorial region, while the cold pool refers to the region between 10°-30°.

The low level stability in the cold pool can be written as $\Delta\theta_C = \theta_{700}^C - T_C$ where $\theta_{700}^C$ is the potential temperature over the cold pool at 700 mb and $T_C$ is the sea surface temperature of the cold pool. Analogously, the low level stability of the warm pool is $\Delta\theta_W = \theta_{700}^W - T_W$ . Since in the tropics the atmosphere can not sustain large temperature gradients there is a nearly uniform horizontal temperature distribution above the trades inversion. Thus, $\theta_{700}^C = \theta_{700}^W$ and the stability of the cold pool can be written as $\Delta\theta_C = \Delta\theta_W + \left(T_W - T_C\right)$ , implying a dependence on the meridional SST difference. The OHT can then affect the low level atmospheric stability and clouds through changes in the meridional SST difference: as OHT decreases the meridional gradient increases and subtropical stability will increase. Since an increase in vertical stability inhibits the entrainment of dry air from above the boundary layer the relative humidity in the boundary layer will increase and more clouds will form. For increased OHT the meridional difference will reduce, and it can become zero in the limit $T_W = T_C$ , i.e. when the tropical region becomes uniformly warm. In this limit the low level stability of equatorial and off-equatorial regions become similar. As discussed above, the physically plausible regimes that are consistent with imposing OHT are for $T_W \geq T_C$ .

Based on this discussion we look at the differences in the tropical response between cases for decreased or increased OHT plotting the spatial distribution of low-level stability ( calculated as the difference between potential temperature at 700 mb and surface temperature) and low clouds. For decreased OHT (c=0.5) the increase in the meridional SST difference leads to an increase in the subtropical stability and the formation of more low clouds, independently on the cloud scheme (Figs. 10c,d; 11c,d). This is accompanied by an equatorward shift of the ITCZ and a strengthening of the Hadley circulation (Fig. 12c,d), as was also reported by H05. Overall, the changes in clouds and atmospheric circulation represent a relatively small deviation from present-day conditions.

For increased OHT (c=1.5) the tropical meridional SST difference becomes negative decreasing the vertical stability between 10°-30°, so that the amount of low clouds decreases, and the stability in the equatorial region increases (Fig. 10e,f; 11e,f). Since for c=1.5 the subtropics are warmer than the equatorial region, the regions of atmospheric ascent change. In this case twin ITCZs develop at about 20°N, S and now subsidence establishes in the equatorial region. Thus, the Hadley circulations reverse (Fig. 12e,f). This equatorial subsidence creates very stable conditions close to the equator leading to a huge increase in the low level clouds, increasing the albedo as we saw above. As the subsidence also inhibits the convective activity, the deep tropical atmosphere becomes very dry as shown in Figure 6. Results using both schemes are similar, but again the tropical circulation changes are largest when the prognostic cloud scheme is used. In particular, in the case of the diagnostic cloud scheme the southern Hadley circulation tends to reverse but is close to zero.

*a. Adjustment*

In order to further understand the processes involved we looked more closely at the initial adjustment of the atmosphere to an increase in OHT for the case of prognostic clouds. We consider the case of c=1.25.

Figure 13a shows the difference in surface temperature with respect to the Control case after 2 years of integration, while Figure 13b shows the temperature changes on years 11-12 of the experiment. Initially the tropical oceans cool uniformly and the high latitudes start to warm (Fig. 13a). After 10 years, the tropics developed a large cooling with an east-west gradient. The high latitudes, on the other hand, have stopped warming and show mainly a small cooling. The adjustment time scale agrees with the one found for the surface fluxes (Fig. 4).

The tropical evolution can be further characterized by the time evolution of the zonal and meridional SST differences (as previously defined for Fig. 9; Fig. 13c), as well as by the evolution of the precipitation in the northern subtropics (Fig. 13d). The meridional SST difference (Fig. 13c, black line) starts to decrease from the beginning of the experiment, and accompanying that evolution precipitation in the region around 20°N starts to increase. After about 2-3 years the meridional difference becomes negative and the precipitation in the northern subtropics is close to its equilibrium value, signaling the development of a northern ITCZ. On the other hand, the equatorial zonal difference (Fig. 13c, red line) only starts to change after year 3 of integration, when it starts to increase, accompanied by a strengthening of the Walker circulation (Fig. 14). Thus, based on these results and those of the previous sections we propose the following chain of events:

1. An increase in OHT leads to a uniform cooling of the equatorial region.
2. At year ~3 the meridional difference becomes negative, meaning that the subtropics are now warmer than the tropics.
3. An ITCZ develops in the subtropics (both at 20°N and 20°S) creating a reverse Hadley cell. The reversed Hadley cell induces subsidence in the equatorial region, and thus increases the stability of the atmospheric column.
4. The increased stability increases the SST-cloud feedback in the equatorial region further cooling the SST, thus increasing the meridional SST gradient.
5. Since subsidence inhibits convection this induces a drying of the deep tropical atmosphere which contributes to the cooling.
6. Since stability is largest in the east, the increase in equatorial low clouds is larger in the east than in the west. This increases the east-west SST gradient, which strengthens the Walker circulation leading to a further increase in vertical stability, low clouds and cooling of the east.

The crucial step in this chain of events is the initial equatorial cooling, which depends on the SST-cloud feedback. If the equatorial region becomes colder than the subtropics, as in the case described here, then the processes described above lead to a solution that is not physically plausible and global cooling. If the equatorial region does not cool that much as in the case for diagnostic clouds (c=1.25) then the meridional difference does not become negative, the solution is physically plausible, and -even though the tropics will cool- the global climate will warm. Overall, the results suggest that the net climate effect of increased OHT will depend on the intensity of the positive feedback between SST and stratus clouds. In our experiments the intensity of that feedback depends on the cloud scheme.

## 6. Summary and discussion

In this work we have studied the climate sensitivity to changes in the ocean heat transport. As in previous studies, we have used an atmospheric general circulation model coupled to a motionless slab ocean where the ocean heat transport can be prescribed. We have examined the response for decreased, as well as for increased ocean heat transport with respect to present-day conditions.

For decreased ocean heat transport we have found very similar results as previously reported by W03 and H05: a decrease in the heat transported by the ocean cools the climate by increasing the sea ice extent and the low oceanic cloud cover, thus increasing the albedo. Moreover, the tropical regions become narrower thus decreasing the moistening of the subtropical atmosphere and thus the greenhouse trapping. These atmospheric changes are such that the atmospheric heat transport tends to compensate for the decreased OHT: there is almost complete compensation in the deep tropics while in the extratropics the total poleward transport of heat is smaller when the ocean circulation is absent. We propose that these changes are robust across models mainly because decreasing the ocean heat transport does not fundamentally alter the circulation of the present-day atmosphere, it essentially represents a small deviation from today's conditions.

The climatic response for larger than present-day values of ocean heat transport is very different from previous studies and it is highly dependent on the parameterization of low clouds. Taking equatorial regions warmer than the subtropics as a plausibility criterion for the solution, the results are that an increase in OHT tends to warm the climate and that this warming is largest when the tropical region is widest. However, the cloud scheme dictates how much can the OHT increase before the solution becomes unphysical. A highly sensitive scheme suggests that our current climate is very close to the maximum positive effect of the ocean heat transport on climate (less than a 15% increase away); another cloud scheme suggests that the climate can further warm 0.6 K for a 25% increase in OHT. For OHT increases larger than 25% of present-day values, a strong positive radiative feedback between tropical low level clouds and sea surface temperature works, always leading to an unphysical cold climate. In this state, low level clouds tend to cover the tropics which increases the albedo enormously. At the same time, the Hadley circulation reverses, inducing subsidence over the tropics which inhibits convection and dries the atmosphere, thus cooling it further due to decreased greenhouse trapping. As a consequence the tropical atmosphere transports heat equatorward resulting in decreased total ocean+atmosphere heat transport when the OHT increases.

Thus, as long as the cloud cover parameterizations are correct, the results presented here do not support the hypothesis that larger OHT may have led in the past to warmer than present-day climates without changing the total poleward heat transport, as has been suggested in the literature. We argue that the results of Barron et al. (1993) are due to the use of an atmospheric model with simpler physical parameterizations. To test this we repeated the experiment of increasing the OHT using the International Centre for Theoretical Physics (ICTP) AGCM, an atmospheric model with an horizontal resolution of T30 and 8 vertical levels and simpler parameterizations of the physical processes (Molteni 2003, Kucharski et al. 2005). In this model cloud cover is defined diagnostically from the values of relative humidity in the air column (excluding the boundary layer) and the total precipitation, and cloud albedo is proportional to the total cloud cover. We found that this model warms 0.8 K when the OHT is increased from 0 to present day values and 0.4 K from present-day to two times present-day heat transport. The sensitivity is much smaller than that of ECHAM5, and even compared to that of the model of Barron et al. (1993). However, as in the latter case, an increase in ocean heat transport always warms the climate, and in a nonlinear way. Taken together, the results of this work suggest that the simpler the cloud cover scheme and the cloud-albedo relationship the less sensitive is the model to changes in ocean heat transport. This is mainly due to differences in the parameterization of low level clouds, and their interaction with radiative fluxes.

A caveat of our results is the lack of ocean dynamical adjustment which may act as a negative feedback opposing cloud-SST feedback that leads to the large simulated tropical cooling, in a similar way as found by Hazeleger et al (2005). Note that this caveat applies not only for increased values of the OHT, but also for decreased values because all solutions involve changes in the surface winds. Other possibilities include that the schemes used in today's models are missing important physics to represent correctly the behavior of low clouds, as has been suggested previously (Bony and Dufresne 2005), and so past climates could be used as test for models.

To date our understanding of the climatic response to changed OHT comes mainly from atmospheric models coupled to fixed oceans (e.g. W03, H05). Our results point that not only is the lack of dynamical adjustment an important issue when using these models, but also the parametrization of low clouds that result in cloud-SST radiative feedbacks of different strengths. In the end, only through the use of coupled models that allow the interaction between these processes will be possible to address this question fully. Nonetheless, we believe the results presented here can serve as a guide for future explorations of the role of the oceans in climate.

**Acknowledgments**

The authors would like to thank Erich Roeckner for his suggestions and encouragement during the course of the study. This work was done during a visit of MB at the Instituto Nazionale di Geofisica e Vulcanologia within the International Program for Advanced Studies on Environment and Climate (PISAC). We are also grateful to the reviewers for their valuable suggestions.

**References**


Abbot D.S., and E. Tziperman, 2008: Sea ice, high-latitude convection, and equable climates. *Geophys. Res. Lett.*, **35**, L03702, doi:10.1029/2007GL032286.

Barreiro M., S.G. Philander, R. Pacanowski, and A. Fedorov, 2006: Simulations of warm tropical conditions with application to middle Pliocene atmospheres. *Clim. Dyn.,* doi:10.1007/s00382-005-0086-4.

Barron E.J., W.H. Peterson, D. Pollard, and S. Thompson, 1993: Past climate and the role of ocean heat transport: model simulations for the cretaceous. *Paleocenog.,* **8**, 785-798.

Barron E.J., 1987: Eocene equator-to-pole surface ocean temperatures: A significant climate problem? *Paleoceanog.,* **2,** 729-739.

Bony S., and coauthors, 2006: How well do we understand and evaluate climate change feedback processes? *J Climate,* **19,** 3445-3482.

Bony S., and J.L. Dufresne, 2005: Marine boundary layer clouds at the heart of tropical cloud feedback uncertainties in climate models. *Geophys. Res. Lett.,* **32**, doi:10.1029/2005GL023851.

Brierley C., A.V. Fedorov, Z. Liu, T. Herbert, K. Lawrence, and J. LaRiviere, 2009: Greatly expanded tropical warm pool and weaker Hadley circulation in the early Pliocene, *Science* **323**, 1714-1718.

Clement A., and R. Seager, 1999: Climate and the tropical oceans. *J. Climate,* 3383-3401.

Dowsett H.J., J.A. Barron, and R. Poore, 1996: Middle Pliocene sea surface temperatures: a global reconstruction. *Mar. Micropaleontol.* **27,** 13-26.

Dowsett H.J., M.A. Chandler, and M.M. Robinson, 2009: Surface temperatures of the Mid-Pliocene North Atlantic Ocean: implications for future climate. *Phil Trans R Soc A,* **367,** 69-84.

Emanuel, K., 2002: A simple model of multiple climate regimes. *J. Geophys. Res.* **107**, doi: 10.1029/2001JD001002.

Enderton, D., and J. Marshall, 2009: Exploration of atmosphere-ocean-ice climates on an aqua-planet and their meridional energy transports. *J. Atmos. Sci.*, 66, 1593-1611.

Fedorov, A.V., P.S. Dekens, M. McCarthy, A.C. Ravelo, P.B. deMenocal, M. Barreiro, R.C. Pacanowski, and S.G. Philander, 2006: The Pliocene Paradox (Mechanisms for a permanent El Niño). *Science,* **312**, 1485-1489.

Hazeleger, W., C. Severijns, R. Seager, and F. Molteni, 2005: Tropical Pacific-Driven decadal energy transport variability. *J. Climate*, **18**, 2037-2051.

Herweijer, C., R. Seager, M. Winton, and A. Clement, 2005: Why ocean heat transport warms the global mean climate. *Tellus,* **57A,** 662-675.

Huber, M., and L.C. Sloan, 2001: Heat transport, deep waters, and thermal gradients: Coupled simulation of an Eocene greenhouse climate. *Geophys. Res. Lett.* **28**, 3481-3484.

Klein, S.A., and D. L. Hartmann, 1993: The seasonal cycle of low stratiform clouds. *J. Climate* **6,** 1587-1606.

Kucharski, F., F. Molteni, and A. Bracco, 2005: Decadal interactions between the western tropical Pacific and the North Atlantic Oscillation, *Clim. Dyn.* doi:10.1007/s00382-005-0085-5.

Lohmann, U., and E. Roeckner, 1996: Design and performance of a new cloud microphysics scheme developed for the ECHAM general circulation model. *Clim. Dyn.* **12,** 557-572.

Miller, R.L., 1997: Tropical thermostats and low cloud cover. *J. Climate,* **10,** 409-440.

Molteni, F., 2003: Atmospheric simulations using a GCM with simplified physical parametrizations. I. Model climatology and variability in multi-decadal experiments. *Clim Dyn* **20,** 175-191.

Rind, D., and M. Chandler, 1991: Increased ocean heat transports and warmer climate. *J. Geophys. Res.* **96,** 7437-7461.

Roeckner E., and co-authors, 2003: The atmospheric general circulation model ECHAM 5. Part I: Model description, *MPI-Report* **349**, 127 pp.

Romanova, V., G. Lohmann, K. Grosfeld, and M. Butzin, 2006: The relative roles of oceanic heat transport and orography on glacial climate. *Quat. Sci. Rev.* **25**, 832-845.

Stone, P.H., 1978: Constraints on dynamical transports of energy on a spherical planet. *Dyn. Atmos. Oceans.,* **2,** 123-139.

Sundqvist. H., E. Berge, and J.E. Kristjansson, 1989: Condensation and cloud parameterization studies with a mesoscale numerical weather prediction model. *Mon. Weather Rev.,* **117,** 1641-1657.

Tompkins, A., 2002: A prognostic parameterization for the subgrid-scale variability of water vapor and clouds in large-scale models and its use to diagnose cloud cover. *J. Atmos. Sci.* **59,** 1917-1942.

Trenberth, K.E., and J.M. Caron, 2001: Estimates of meridional atmosphere and ocean heat transports. *J. Climate,***14**, 3433-3443.

Vecchi, G.A., B.J. Soden, A.T. Wittenberg, I.M. Held, A. Leetma, and M.J. Harrison, 2006: Weakening of tropical Pacific atmospheric circulation due to anthropogenic forcing. *Nature* **441,** 73-76.

Winton, M., 2003: On the climatic impact of ocean circulation. *J. Climate,* **16,** 2875-2889.

Zachos, J.C., and L.D. Scott, K.G. Lohmann,1994: Evolution of early Cenozoic marine temperatures. *Paleoceanography*, **9**, 353-387.

**Figure Captions**

**Figure 1-** Spatial structure of the net surface heat flux (same as ocean heat transport in steady state) in $W/m^2$ for the c=1.5 experiment with prognostic clouds.

**Figure 2-** a) Global mean surface temperature (°C), b) top of the atmosphere global mean radiation balance terms: shortwave (solid), longwave (dashed) radiations ($W/m^2$), and c) total cloud cover (as fraction), as function of ocean heat transport strength. Results are shown for both prognostic (black) and diagnostic (red) cloud schemes. A value of c>1 indicates increased oceanic heat transport, while a value of c<1 indicates reduced oceanic heat transport with respect to present-day (Control) conditions.

**Figure 3-** Surface temperature (°C) (upper panels) and difference (°C) with respect to Control (lower panels) for (a,c) c=0.5 (50% OHT decrease) experiment, and (b,d) c=1.5 (50% OHT increase) experiment, using prognostic clouds.

**Figure 4-** Surface heat budget terms of the Pacific cold tongue region (corresponding to the area [120°W-90°W, 5°S-5°N]) for experiments using the prognostic clouds. a) Latent heat, b) sensible heat, c) net shortwave radiation, and d) net longwave radiation. Fluxes are in $W/m^2$ and are positive downward. Three cases are shown: Control (c=1, black), c=0.5 (blue) and c=1.5 (red).

**Figure 5-** Experiment minus Control (c=1) changes for a) shortwave radiation reflected at TOA ($W/m^2$), b) upward shortwave radiation at the surface ($W/m^2$), c) low level clouds (fraction), and d) fractional sea ice cover. The color code is c = 0, 0.5, 0.75, 1.25, 1.5, 2.

Low level clouds are defined as those within the layer 1000-700mb.

**Figure 6-** Experiment minus Control (c=1) changes for a) total greenhouse trapping ($W/m^2$, defined as difference between the upward longwave radiation at the surface and that at the top of the atmosphere), b) total column water vapor content ($kg/m^2$), c) clear-sky greenhouse trapping ($W/m^2$), and d) total-(clear-sky) greenhouse trapping ($W/m^2$). The color code is c = 0, 0.5, 0.75, 1.25, 1.5, 2.

**Figure 7-** a) Total, b) oceanic, and c) atmospheric heat transport (PW=$10^{15}$ W) for different experiments using the prognostic cloud scheme. The color code is: c = 0, 0.5, 0.75, 1, 1.25, 1.5, 2(marks). The oceanic heat transports is calculated using surface heat fluxes, the total heat transport is derived using top of the atmosphere radiation fluxes and the atmospheric heat transport is the difference between these two. Note that for the case of c=0 there is a remanent of OHT because the model has not yet reach equilibrium.

**Figure 8-** Surface temperature difference (°C) with respect to Control for (a) c=0.5 (50% OHT decrease) experiment, and (b) c=1.5 (50% OHT increase) experiment, using diagnostic clouds.

**Figure 9-** Values of the a) zonal SST difference,(°C) and b) of the meridional SST difference (°C) in the tropical Pacific. The zonal difference is calculated as the SST average over [150°E-165°E,5°S-5°N] minus that over [100°W-85°W,5°S-5°N], while the meridional difference is the SST average over [120°E-100°W,10°S-10°N] minus that over [120°E-100°W,10°N-30°N]. Results for prognostic clouds are in black, and for diagnostic

clouds are in red.

**Figure 10-** Low level atmospheric stability (°C, left panels) and low level clouds (%, right panels) for a,b) c=1 (Control), c, d) c=0.5 (50% reduction of OHT), and e,f) c=1.5 (50% increase of OHT) for experiments using prognostic clouds. The low level stability is calculated as the difference between potential temperature at 700 mb and surface temperature.

**Figure 11-** Same as Fig 10, but for diagnostic clouds.

**Figure 12-** Mean atmospheric mass streamfunction (1e10 kg/s) for c=1 (Control, upper panels), c=0.5 (middle panels), and c=1.5 (lower panels), using the prognostic cloud scheme (left), and diagnostic scheme (right).

**Figure 13-** Changes in surface temperature (°C) a) after first 2 years, and b) for years 11-12 of the experiment with c=1.25 and prognostic cloud scheme compared to the Control (c=1) case. Evolution of c) meridional (black) and zonal (red) SST differences (°C) in the tropical Pacific (as defined in Fig. 9), d) precipitation (kg $m^{-2}s^{-1}$) in the tropical Pacific averaged between [120°E-80°W, 15°N-25°N]. In c) and d) only the first 20 years of the run are plotted.

**Figure 14-** Walker circulation index calculated as the SLP difference between the averages over regions defined by [160°W-80°W, 5°S-5°N] and [80°E-160°E, 5°S-5°N] following Vecchi et al (2006). Positive values indicate a strengthened Walker circulation. We consider prognostic clouds and the black line is for the Control experiment (c=1), while the red line

is for the first 20 years of experiment with c=1.25.

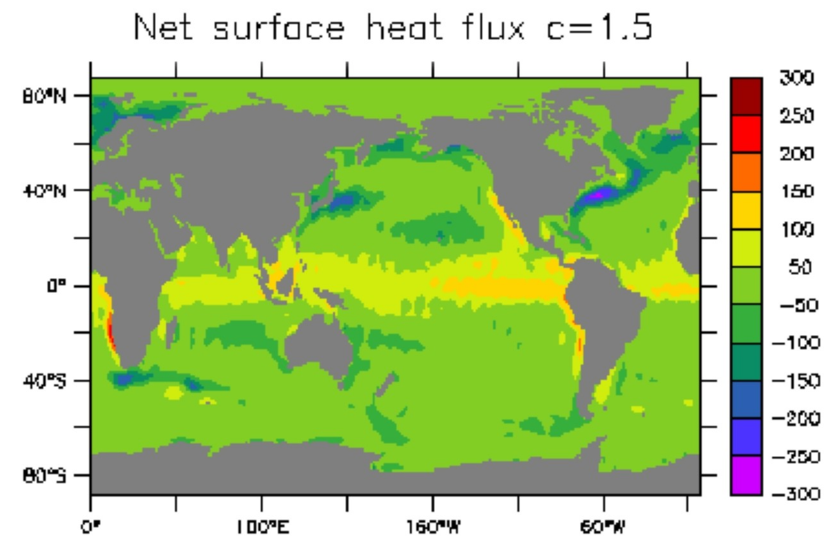
Net surface heat flux c=1.5
80°N
40°N
0°
40°S
80°S
0°
100°E
160°W
60°W
300
250
200
150
100
50
−50
−100
−150
−200
−250
−300

Figure 1

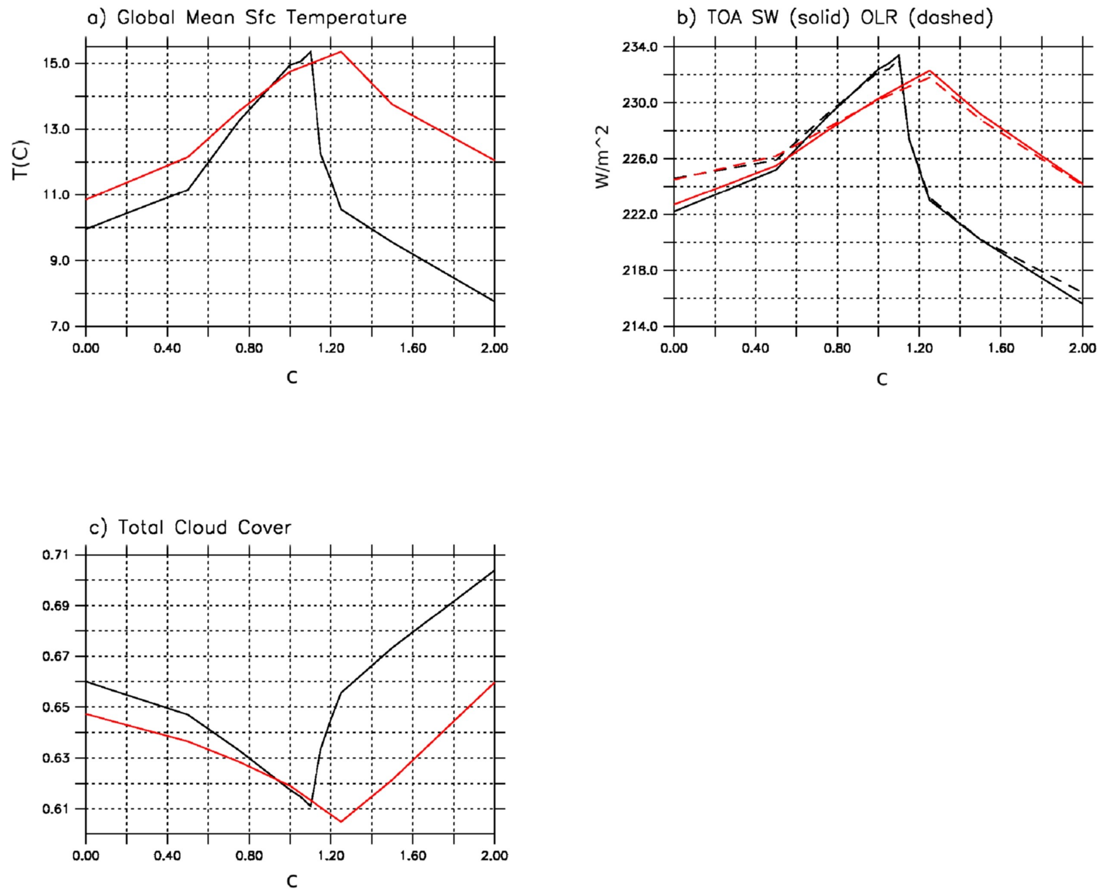
a) Global Mean Sfc Temperature
T(C)
15.0
13.0
11.0
9.0
7.0
0.00
0.40
0.80
1.20
1.60
2.00
c
b) TOA SW (solid) OLR (dashed)
W/m^2
234.0
230.0
226.0
222.0
218.0
214.0
0.00
0.40
0.80
1.20
1.60
2.00
c
c) Total Cloud Cover
0.71
0.69
0.67
0.65
0.63
0.61
0.00
0.40
0.80
1.20
1.60
2.00
c

Figure 2

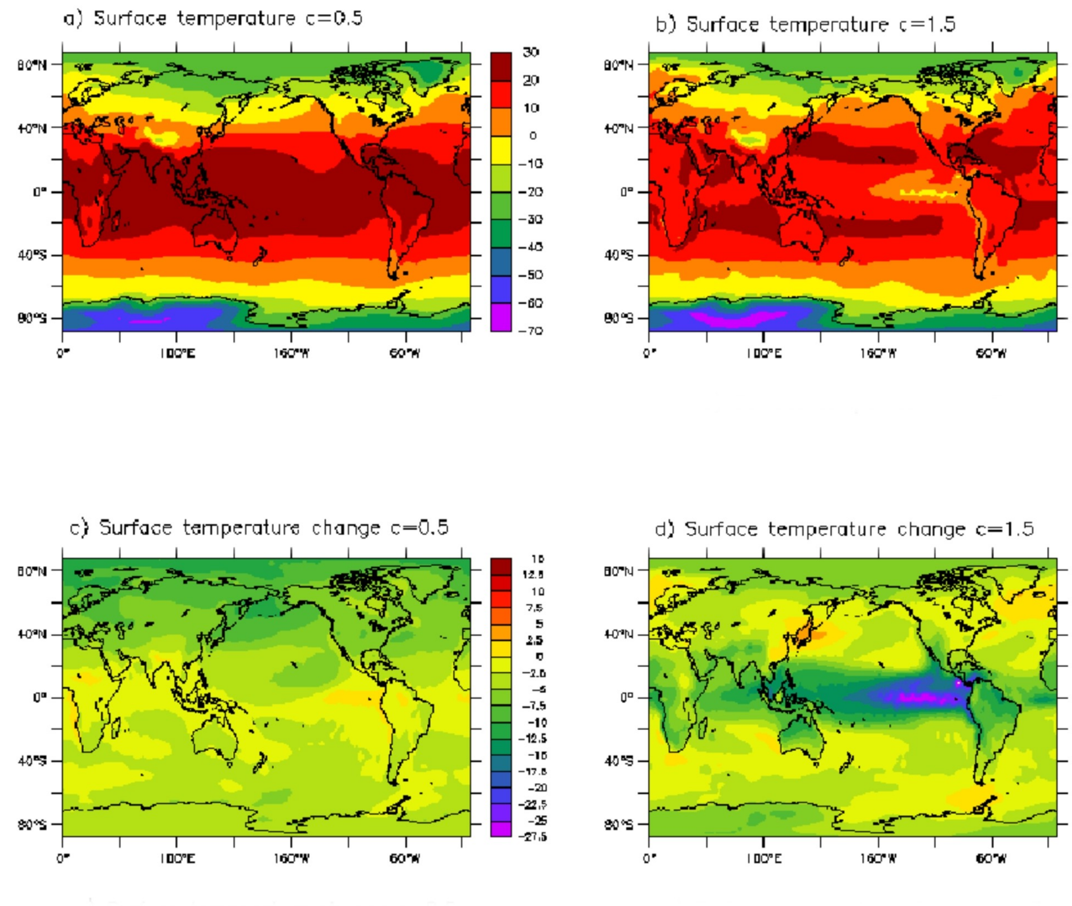
a) Surface temperature c=0.5
b) Surface temperature c=1.5
c) Surface temperature change c=0.5
d) Surface temperature change c=1.5
80°N
40°N
0°
40°S
80°S
0°
100°E
160°W
60°W
30 20 10 0 -10 -20 -30 -40 -50 -60 -70
15 12.5 10 7.5 5 2.5 0 -2.5 -5 -7.5 -10 -12.5 -15 -17.5 -20 -22.5 -25 -27.5

Figure 3

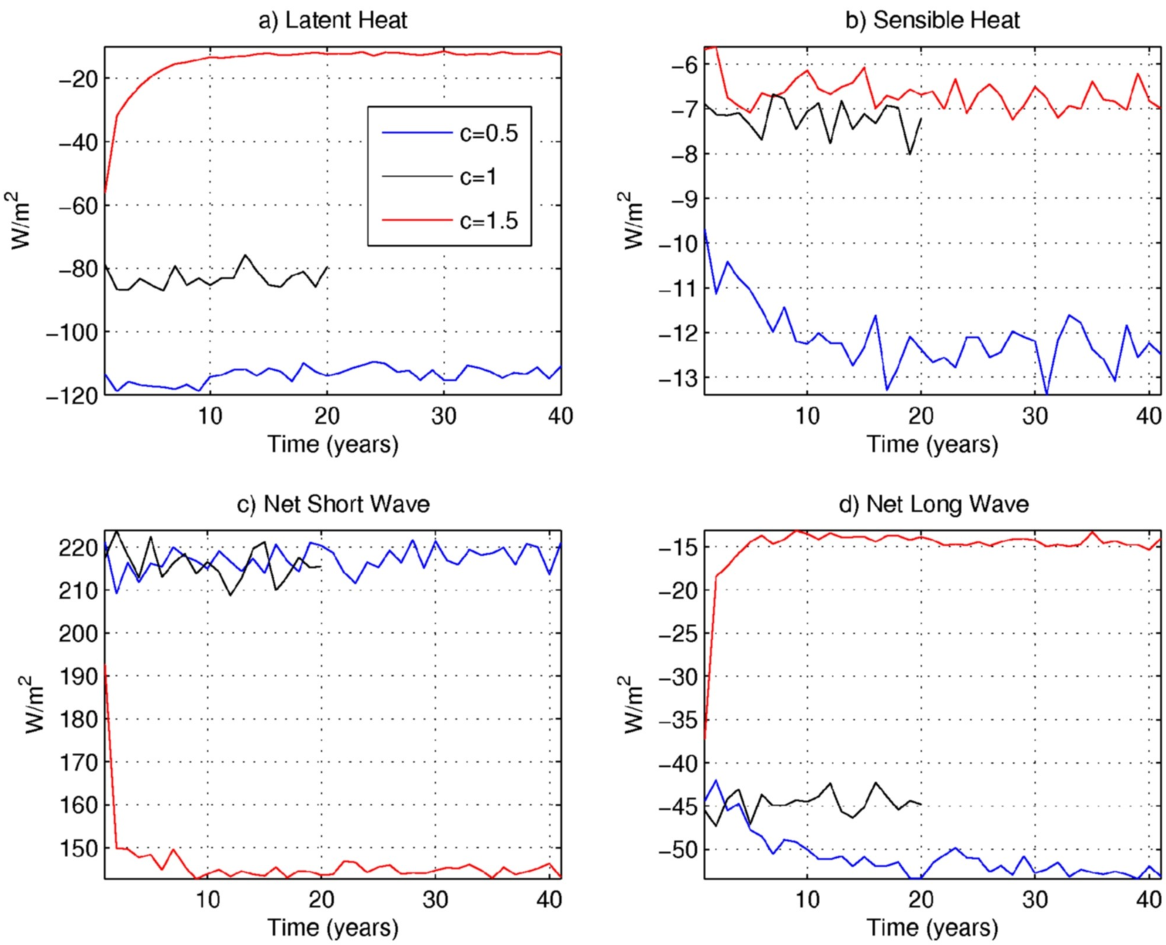
a) Latent Heat
b) Sensible Heat
c) Net Short Wave
d) Net Long Wave
c=0.5
c=1
c=1.5
W/m$^2$
Time (years)

Figure 4

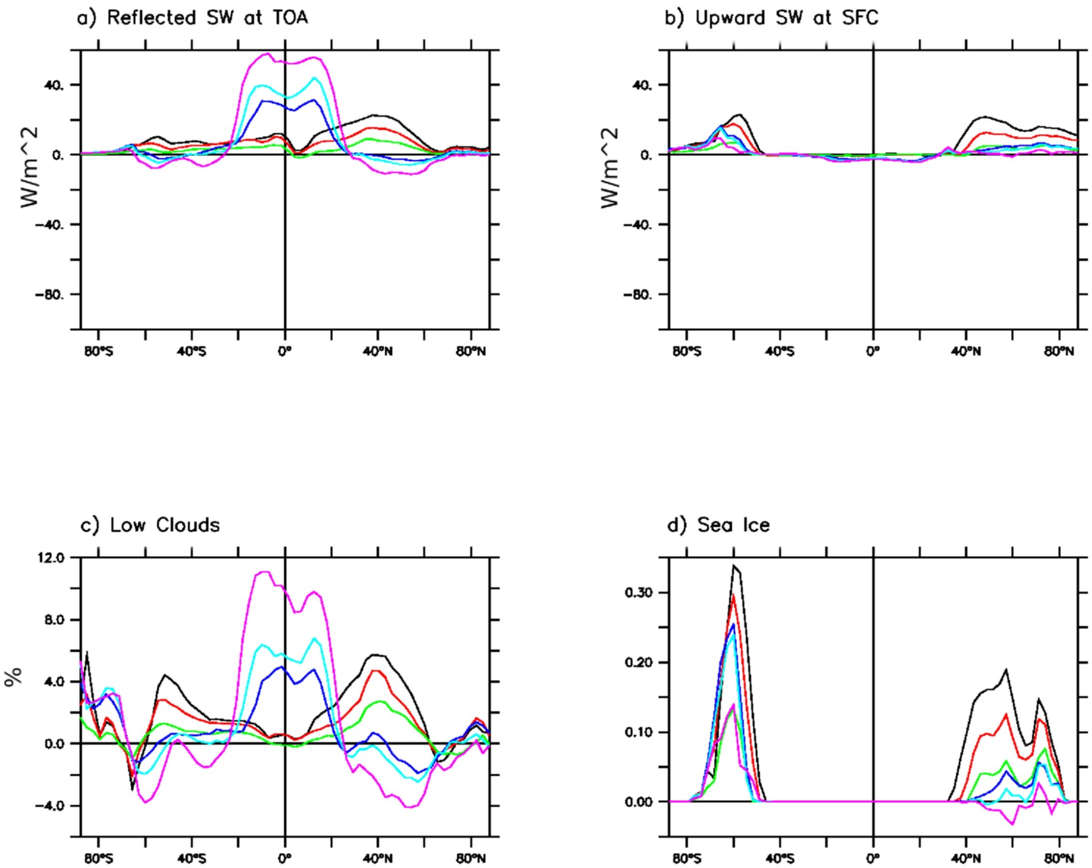

a) Reflected SW at TOA
b) Upward SW at SFC
c) Low Clouds
d) Sea Ice
W/m^2
W/m^2
%
40.
0.
-40.
-80.
12.0
8.0
4.0
0.0
-4.0
0.30
0.20
0.10
0.00
80°S
40°S
0°
40°N
80°N


Figure 5

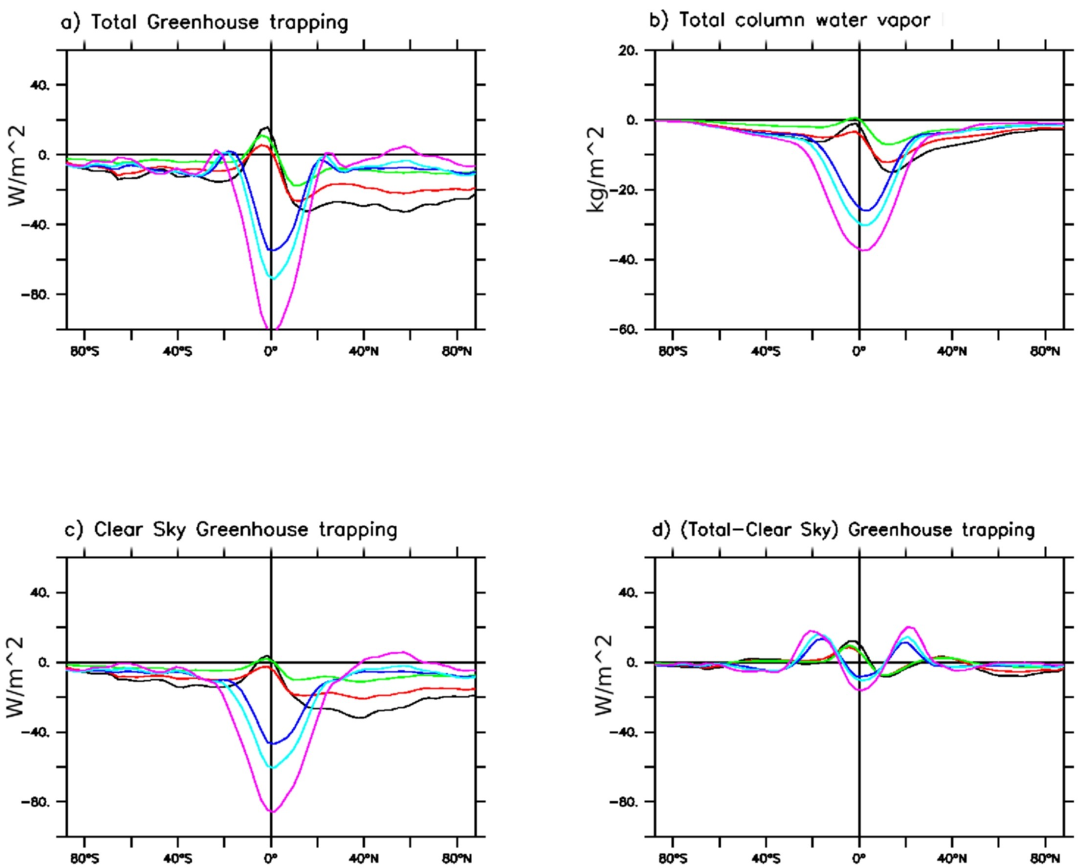
a) Total Greenhouse trapping
W/m^2
40.
0.
-40.
-80.
80°S
40°S
0°
40°N
80°N
b) Total column water vapor
kg/m^2
20.
0.
-20.
-40.
-60.
80°S
40°S
0°
40°N
80°N
c) Clear Sky Greenhouse trapping
W/m^2
40.
0.
-40.
-80.
80°S
40°S
0°
40°N
80°N
d) (Total-Clear Sky) Greenhouse trapping
W/m^2
40.
0.
-40.
-80.
80°S
40°S
0°
40°N
80°N

Figure 6

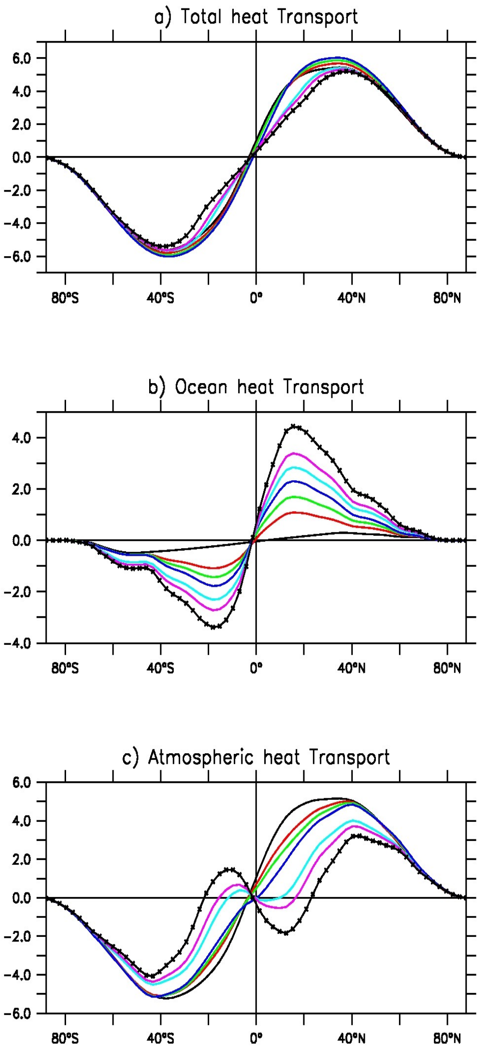
a) Total heat Transport
6.0
4.0
2.0
0.0
−2.0
−4.0
−6.0
80°S
40°S
0°
40°N
80°N
b) Ocean heat Transport
4.0
2.0
0.0
−2.0
−4.0
80°S
40°S
0°
40°N
80°N
c) Atmospheric heat Transport
6.0
4.0
2.0
0.0
−2.0
−4.0
−6.0
80°S
40°S
0°
40°N
80°N

Figure 7

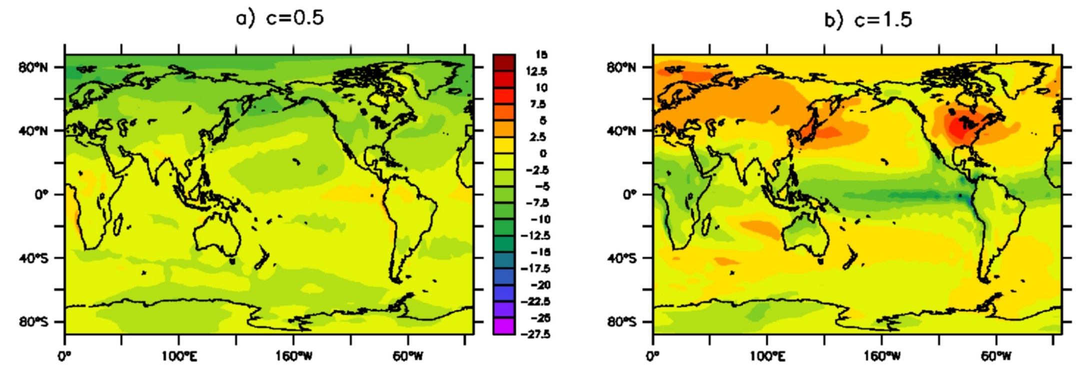
a) c=0.5
b) c=1.5
80°N
40°N
0°
40°S
80°S
0°
100°E
160°W
60°W
15
12.5
10
7.5
5
2.5
0
-2.5
-5
-7.5
-10
-12.5
-15
-17.5
-20
-22.5
-25
-27.5

Figure 8

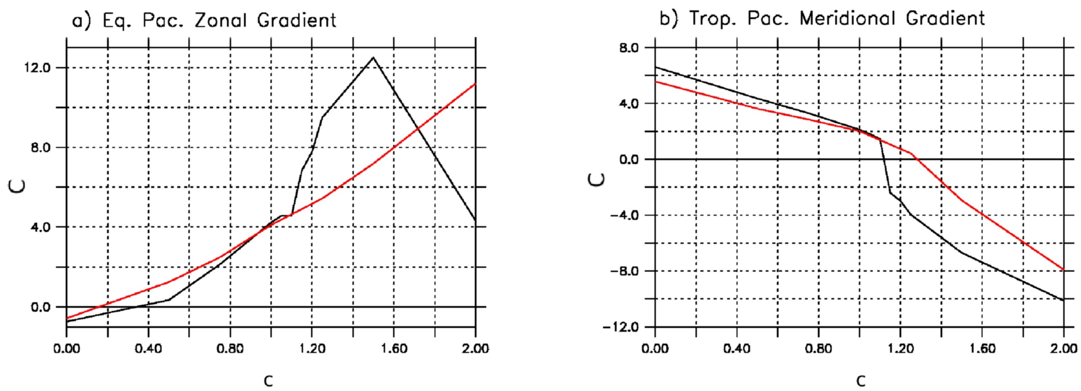
a) Eq. Pac. Zonal Gradient
b) Trop. Pac. Meridional Gradient
C
c
12.0
8.0
4.0
0.0
-4.0
-8.0
-12.0
0.00
0.40
0.80
1.20
1.60
2.00

Figure 9

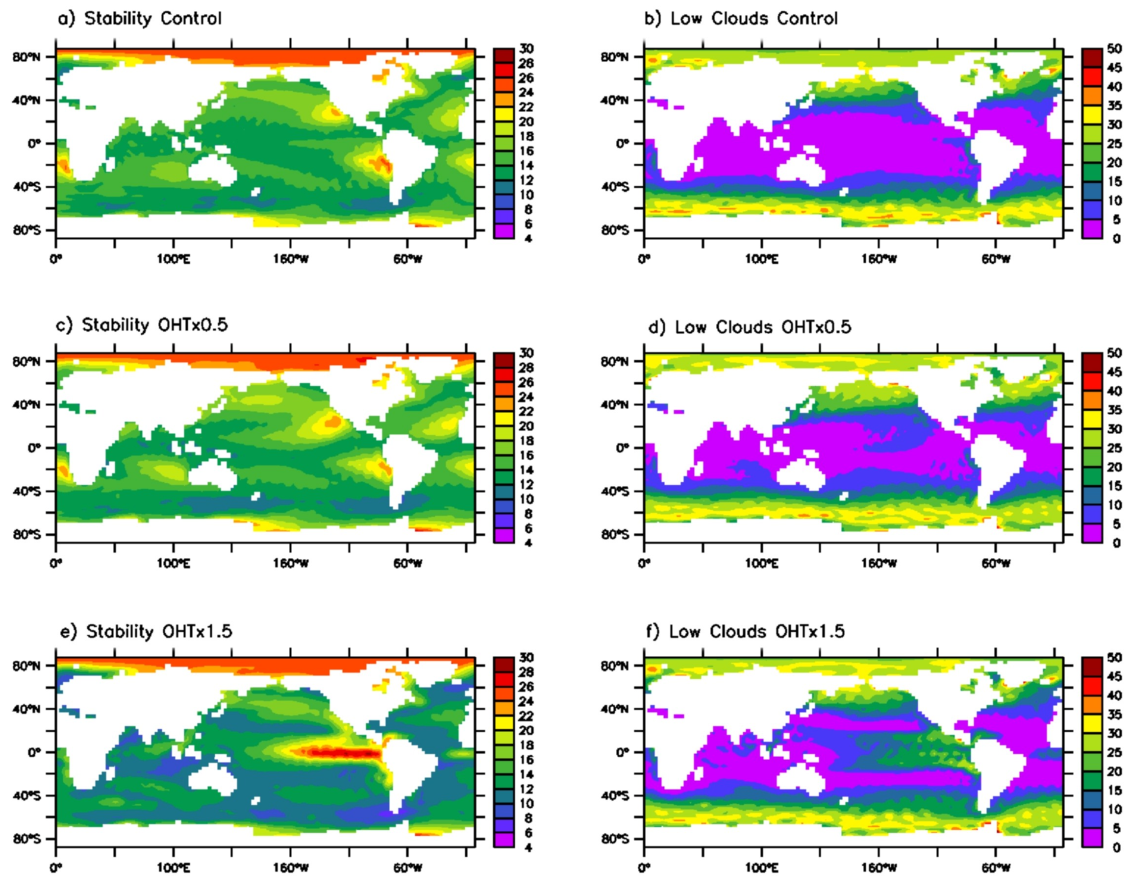
a) Stability Control
b) Low Clouds Control
c) Stability OHTx0.5
d) Low Clouds OHTx0.5
e) Stability OHTx1.5
f) Low Clouds OHTx1.5
80°N
40°N
0°
40°S
80°S
0°
100°E
160°W
60°W
4 6 8 10 12 14 16 18 20 22 24 26 28 30
0 5 10 15 20 25 30 35 40 45 50

Figure 10

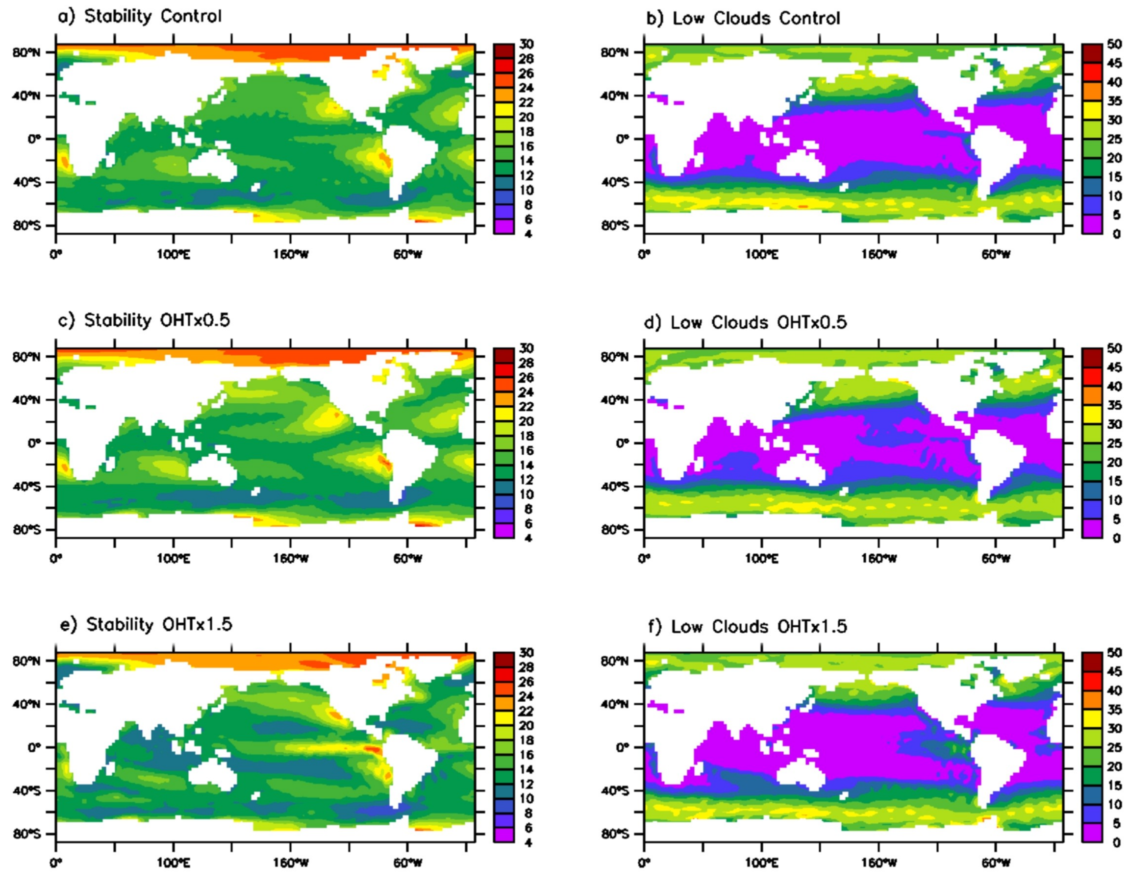
a) Stability Control
b) Low Clouds Control
c) Stability OHTx0.5
d) Low Clouds OHTx0.5
e) Stability OHTx1.5
f) Low Clouds OHTx1.5
80°N
40°N
0°
40°S
80°S
0°
100°E
160°W
60°W
30 28 26 24 22 20 18 16 14 12 10 8 6 4
50 45 40 35 30 25 20 15 10 5 0

Figure 11

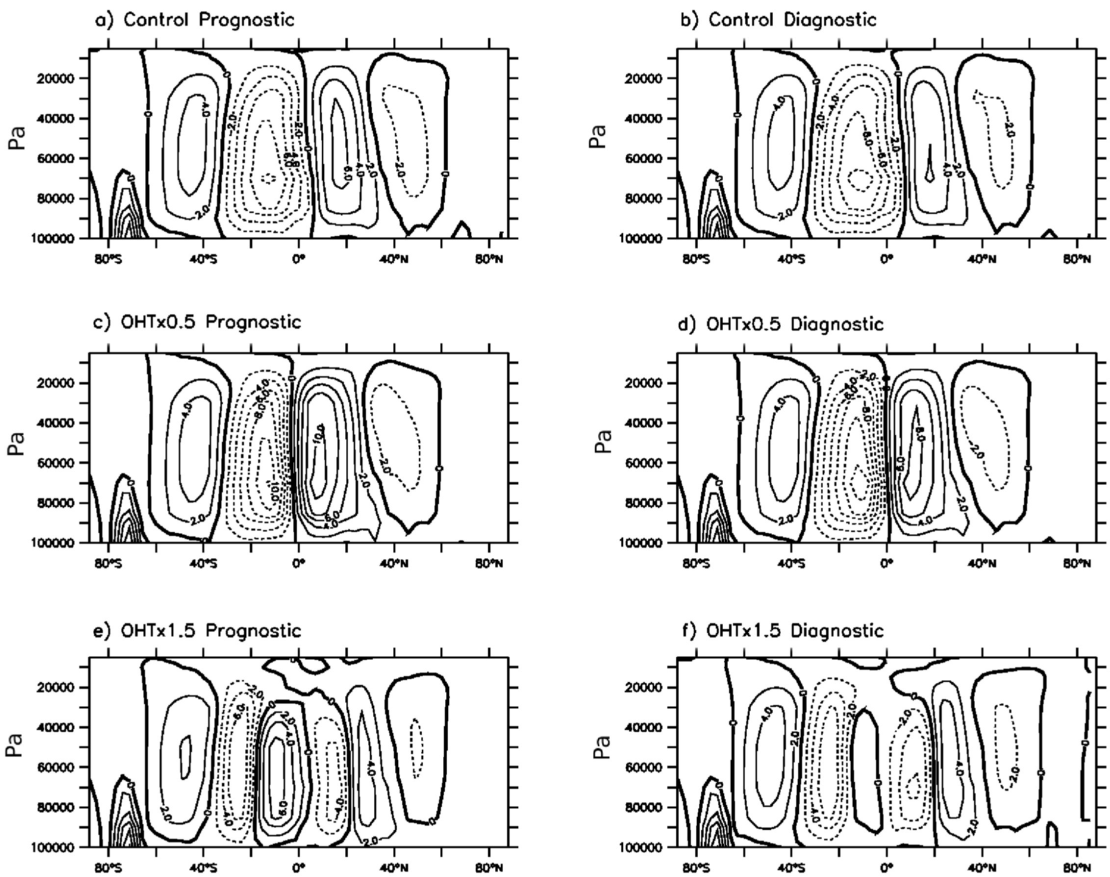
a) Control Prognostic
b) Control Diagnostic
c) OHTx0.5 Prognostic
d) OHTx0.5 Diagnostic
e) OHTx1.5 Prognostic
f) OHTx1.5 Diagnostic
Pa
20000
40000
60000
80000
100000
80°S
40°S
0°
40°N
80°N

Figure 12

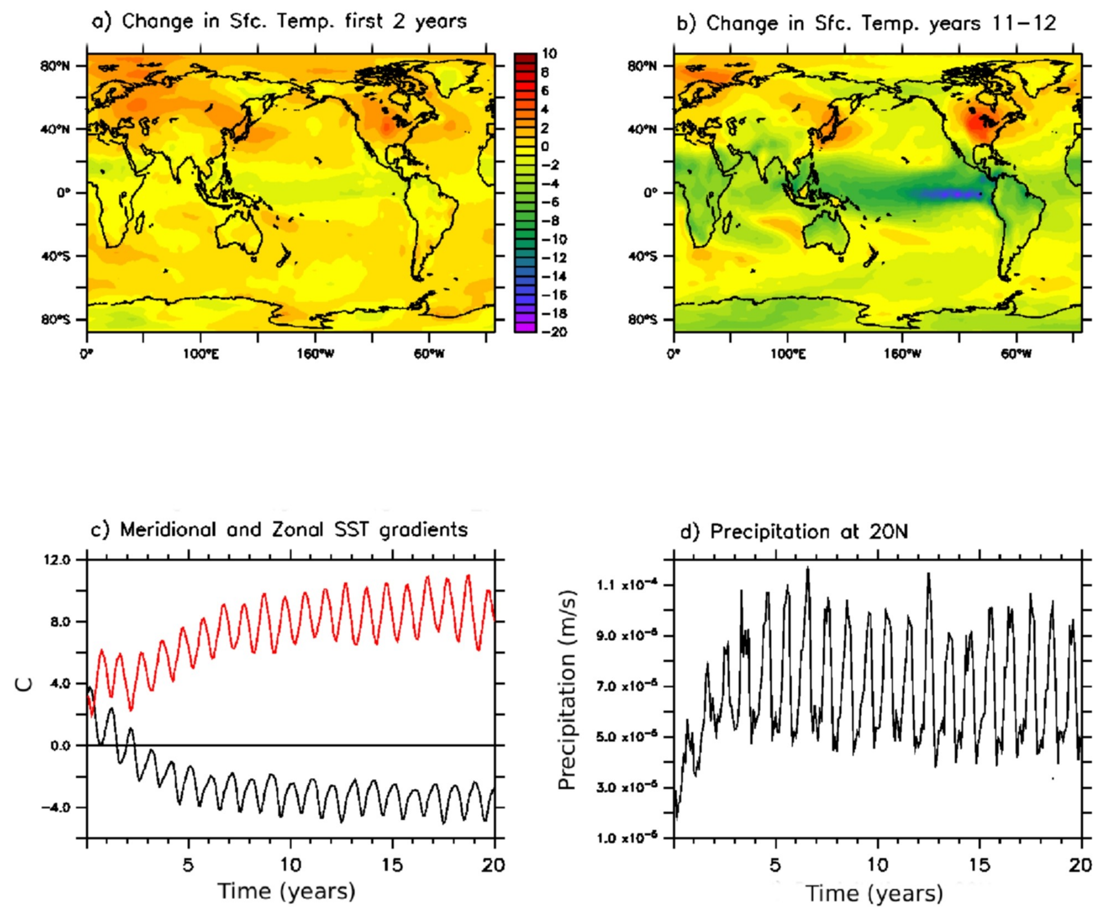
a) Change in Sfc. Temp. first 2 years
b) Change in Sfc. Temp. years 11−12
80°N
40°N
0°
40°S
80°S
0°
100°E
160°W
60°W
10
8
6
4
2
0
−2
−4
−6
−8
−10
−12
−14
−16
−18
−20
c) Meridional and Zonal SST gradients
C
12.0
8.0
4.0
0.0
−4.0
5
10
15
20
Time (years)
d) Precipitation at 20N
Precipitation (m/s)
1.1 x10−4
9.0 x10−5
7.0 x10−5
5.0 x10−5
3.0 x10−5
1.0 x10−5
5
10
15
20
Time (years)

Figure 13

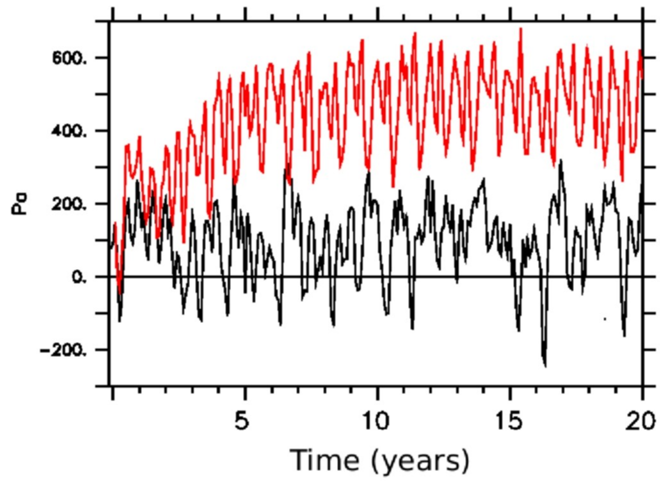


Figure 14